International Telecommunication Union

ITU-R

Radiocommunication Sector of ITU

Report ITU-R RA.2507-0
(10/2022)

Technical and operational characteristics of the existing and planned Geodetic Very Long Baseline Interferometry

RA Series

Radio astronomy

International Telecommunication Union

Foreword

The role of the Radiocommunication Sector is to ensure the rational, equitable, efficient and economical use of the radio-frequency spectrum by all radiocommunication services, including satellite services, and carry out studies without limit of frequency range on the basis of which Recommendations are adopted.

The regulatory and policy functions of the Radiocommunication Sector are performed by World and Regional Radiocommunication Conferences and Radiocommunication Assemblies supported by Study Groups.

Policy on Intellectual Property Right (IPR)

ITU-R policy on IPR is described in the Common Patent Policy for ITU-T/ITU-R/ISO/IEC referenced in Resolution ITU-R 1. Forms to be used for the submission of patent statements and licensing declarations by patent holders are available from http://www.itu.int/ITU-R/go/patents/en where the Guidelines for Implementation of the Common Patent Policy for ITU-T/ITU-R/ISO/IEC and the ITU-R patent information database can also be found.

Series of ITU-R Reports

(Also available online at http://www.itu.int/publ/R-REP/en)

Series	Title
BO	Satellite delivery
BR	Recording for production, archival and play-out; film for television
BS	Broadcasting service (sound)
BT	Broadcasting service (television)
F	Fixed service
M	Mobile, radiodetermination, amateur and related satellite services
P	Radiowave propagation
RA	**Radio astronomy**
RS	Remote sensing systems
S	Fixed-satellite service
SA	Space applications and meteorology
SF	Frequency sharing and coordination between fixed-satellite and fixed service systems
SM	Spectrum management

***Note**: This ITU-R Report was approved in English by the Study Group under the procedure detailed in Resolution ITU-R 1.*

Electronic Publication
Geneva, 2022

REPORT ITU-R RA.2507-0

Technical and operational characteristics of the existing and planned Geodetic Very Long Baseline Interferometry

(2022)

TABLE OF CONTENTS

1 Introduction

The purpose of this Report is to provide the technical and operational characteristics of the existing and planned Geodetic Very Long Baseline Interferometry (VLBI) network. VLBI is the foremost observation technique for producing high-accuracy reference frames. High angular resolution is of fundamental importance for the realization of space-fixed and Earth-fixed reference systems as well as for the determination of current Earth orientation parameters (EOP). Reliable and precise reference frames and EOP are fundamental for accurate positioning used in navigating in space and on Earth, mapping, locating frontiers and borders, managing land boundaries, as well as in research and science.

Geodetic Astronomy applies the radio astronomical VLBI method using cosmic extragalactic radio sources as celestial reference points to monitor the orientation of the Earth and to determine terrestrial reference points. The Geodetic VLBI technique has provided essential observational data for decades with milli-meter accuracy. Monitoring EOP is essential to maintain Global Navigation Satellite Systems (GNSS) and to provide precise positioning in space and time. The International VLBI Service for Geodesy and Astrometry (IVS)[1] uses VLBI on a daily basis to generate and provide its products (e.g. Earth rotation parameters and site coordinates) to the International Earth Rotation and Reference System Service (IERS), to space agencies/industry, to satellite operators, to public administrations, and to scientific institutions. Demands on precise positioning for many applications has led to a recently revised Global Geodetic Reference Frame (GGRF) accuracy goal of 1 mm and encouragement for administrations and international organizations to work together to enhance global cooperation in providing technical assistance with the aim of "ensuring development, sustainability and advancement of the global geodetic reference frame" based on UN-GA Resolution 69/266.[2]

The planned Geodetic VLBI networks described in this report are multi-national efforts underway to meet the 1 mm accuracy goal. The globally well-distributed network of VGOS stations, which are expected eventually to number ~40, are passive receivers. While originally built with narrow-bandwidths, the new systems are designed to operate wider bandwidths in the 2-14 GHz range. This wider bandwidth includes specific bands with radio astronomy service (RAS) allocations or existing footnotes recognizing the operation of the radio astronomy service. The frequency bands with RAS allocations includes 2 655-2 700 MHz, 4 800-5 000 MHz, and 10.6-10.7 GHz range, as well as frequency ranges identified by footnote RR No. **5.149**, including 3 260-3 267 MHz, 3 332-3 339 MHz, 3 345.8-3 352.5 MHz, 4 825-4 835 MHz, and 6 650-6 675.2 MHz bands. Further, observations are undertaken in other spectrum bands in the 2-14 GHz range without a radio astronomy allocation on an opportunistic basis, subject to not claiming interference protection. The Geodetic VLBI system is heading towards 24 hours/day and 7 days/week operation, making a series of short observations of faint natural radio sources (e.g. galaxies with radio emission) at different places in the sky. Observations of large numbers of cosmic background sources increase the accuracy of the reference frame; therefore, a low-noise environment is critical as many natural radio sources are faint.

In § 2, the relationship between the VLBI service for geodesy and astrometry is described, as well as a summary of other radiocommunication services relying on the GGRF. Section 3 contains a summary of the legacy and planned upgrades to the VLBI Global Observing System (VGOS). Section 4 contains additional technical details of the VGOS system, including information about the site locations, the wideband receivers, the calibration system, infrastructural requirements, and details on the channels for the frequency setup. Section 5 discusses strategies to maximize system performance and provides the mathematical background to calculate noise levels detrimental to the VGOS goals. Section 6 contains a brief summary.

---

[1] http://ivscc.gsfc.nasa.gov

[2] https://undocs.org/en/A/RES/69/266

2 VLBI service for geodesy and astrometry

Founded in 1999, the International VLBI Service for Geodesy and Astrometry (IVS) is a collaboration of organizations performing global VLBI observations in a service environment on a non-profit basis primarily for the determination of EOP and geodetic reference frames. IVS is a service of the International Astronomical Union (IAU) and of the International Association of Geodesy (IAG). The IAG is establishing the Global Geodetic Observing System (GGOS) to which the IVS is contributing with its VGOS as a key element. The IVS is supported by member institutions such as space agencies, mapping agencies, research institutes, and universities that are committed to provide geodetic and astrometric information.

A global approach to VLBI activities is needed to achieve the accuracy required for optimal state-of-the-art determinations of EOP and reference frames. With this mission and due to its global nature, the IVS promotes synergies for technological developments and the necessary compatibility of standardized equipment and procedures. Individual institutions or even nations are not able to achieve this alone.

The technical and operational parameters of geodetic VLBI are similar to those required by radio astronomy. Both make use of large reflector antennas (radio telescopes) combined with low-noise receivers (front-ends) and high throughput signal processing systems (back-ends) to record and detect faint cosmic signals. Their main characteristics are described in more detail in the next two sections.

2.1 VLBI for astrometry

Astrometry is the science of positional accuracy, with efforts to precisely measure the locations and motion of celestial objects in the plane of the sky. According to Resolution B2 of the International Astronomical Union General Assembly (1997), the fundamental reference system for astronomical applications is identified as the International Celestial Reference Frame (ICRF). The ICRF is space-fixed and is presently based on high accuracy positions of extragalactic radio sources measured by VLBI observation programmes of the IVS. The ICRF is indispensable for accurate space navigation by satellite operators and space agencies.

2.2 VLBI for geodesy

Geodetic VLBI builds on the ICRF established by astrometric VLBI and provides the information about the Earth’s location in space-time. Geodetic VLBI is the only technique to observe the phase of Earth rotation with respect to the coordinated universal time (UTC). This offset, UT1-UTC (see Fig. 1), is important for accurate orbit determinations of space and satellite missions such as the GNSS, which include Global Positioning System (GPS), Global Navigation Satellite System (GLONASS), Beidou, and Galileo. The IVS provides the infrastructure to sustainably maintain the delivery of this product. Furthermore, the geodetic VLBI observations are the only means for tying the global terrestrial reference frame (TRF) to the celestial reference frame (CRF) by the full set of EOP, which includes two polar motion components, UT1-UTC, and two nutation components (see Fig. 1). It should be emphasized here that CRF, EOP, and TRF are mutually dependent in this entire geometric triple with VLBI being the only technique to determine the CRF in the radio frequency domain.

FIGURE 1

Geodetic VLBI is the only means of tying the terrestrial reference frame to the celestial reference frame

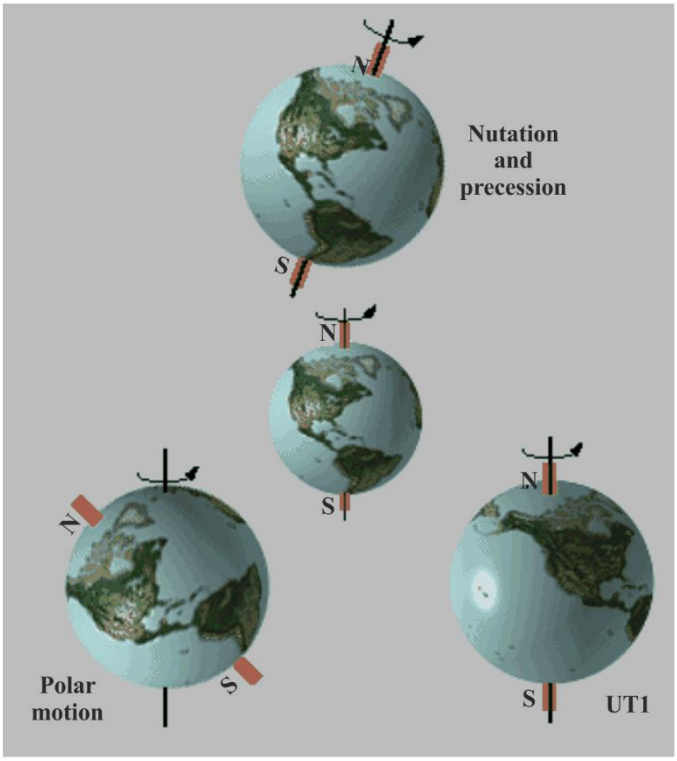

Report RA.2507-01

The TRF, which incorporates results also from other space-geodetic observing techniques GNSS, Satellite Laser Ranging (SLR), and Doppler Orbitography and Radiopositioning Integrated by Satellite (DORIS), includes precise coordinates and velocities of IVS radio telescopes. Here, the IVS strives for 1 mm position accuracy and 0.1 mm/yr velocity accuracy to provide the needed information for Global Change studies regarding climate, plate tectonics, and water cycle in general, and for monitoring global sea level change in particular (see Figs 2 and 3).

Beyond providing positions and velocities of individual sites in the TRF of the IVS, VLBI is one of two backbone techniques for determining the scale parameter of the International Terrestrial Reference Frame (ITRF), which is the basis for many global and regional applications.

Figure 2 illustrates how important high-level scientific questions such as sea level change and weather/climate build upon the geodetic VLBI infrastructure.

FIGURE 2

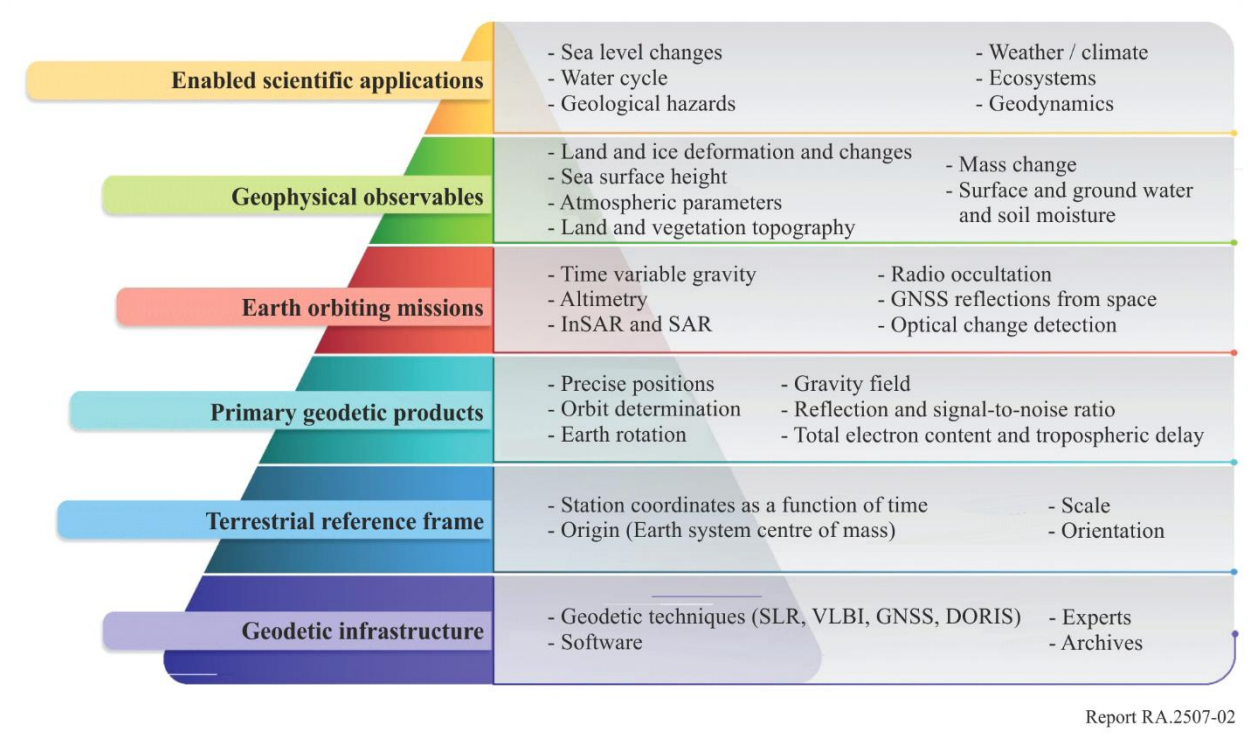

Report RA.2507-02

FIGURE 3

Required positional accuracy to maintain and enhance scientific questions in the areas of ecosystems, weather climate, the water cycle, geological hazards and sea-level change

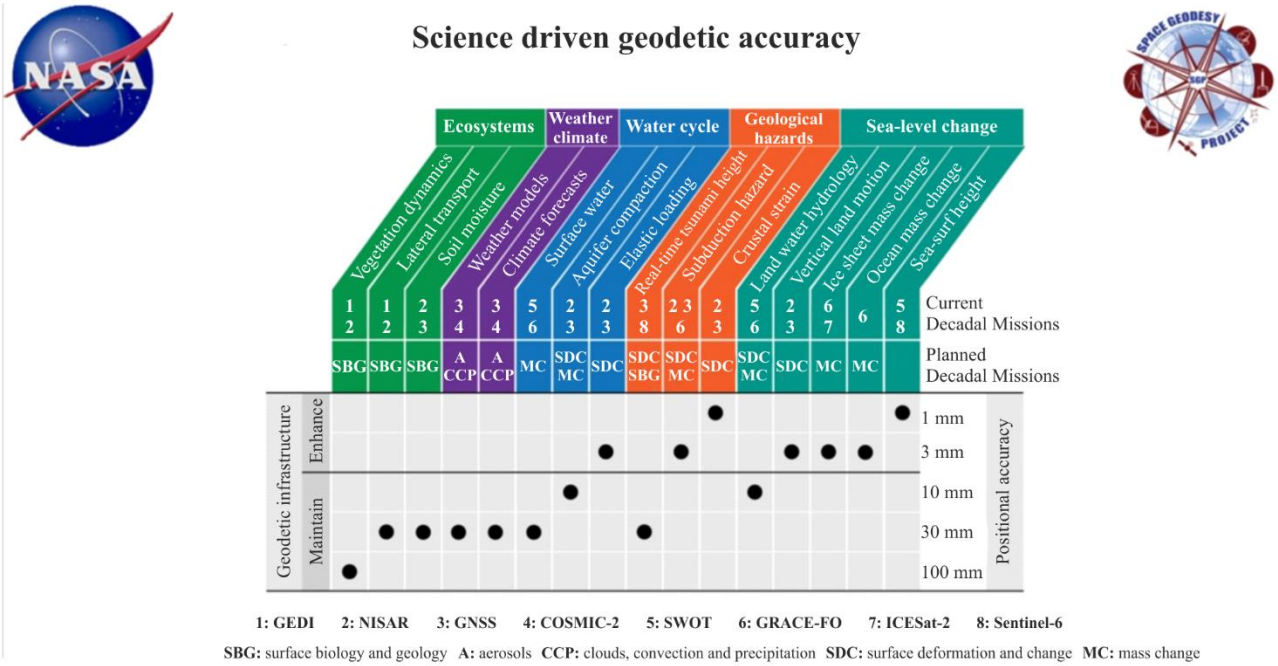

Report RA.2507-03

2.2.1 Services relying on and utilizing the Global Geodetic Reference Frame (GGRF)

Simplified communication models contain a transmitter and a receiver. To make the communication between spatially separated transmitter and receiver happen, the positions and the direction of the transmission are important. If the target position is unknown or time variable and not considered, the

communication is likely to fail. The GGRF is fundamental to applications like GNSS as well as other radio services which makes the GGRF available to many users. Table 1 indicates the general dependency and utilization of the global geodetic reference frame upon radiocommunication services. The dependency is classified by:

– 'high', when most precise positions are required from the GGRF,

– 'normal', when moderate position precision is required,

– '-', when nearly no dependency exists.

In general, it can be concluded that any fast-moving transmitters/receivers on land or in space are very dependent on the precise GGRF in order to target the receiver or track a source. In contrast, slow moving objects (ships) do not require such precise reference frames as satellites for communications, but for the purpose of precise navigation they do.

TABLE 1

Radiocommunication Services and their general dependency on the GGRF (As communication consists of transmitter and receiver, the knowledge of their positions provided by the GGRF is required by most services)

ITU Radio Regulations		GGRF	
No.	**Service (Chapter I, Section III)**	**Dependency**	**Utilization**
1.20	fixed service	–	positions
1.21	fixed-satellite service	high	positions
1.22	inter-satellite service	high	positions
1.23	space operation service	high	positions
1.24	mobile service	normal	positions
1.25	mobile-satellite service	high	positions
1.26	land mobile service	normal	positions
1.27	land mobile-satellite service	high	positions
1.28	maritime mobile service	normal	positions
1.29	maritime mobile-satellite service	normal	positions
1.30	port operations service	–	positions
1.31	ship movement service	–	positions
1.32	aeronautical mobile service	normal	positions
1.33	aeronautical mobile route service	normal	positions
1.34	aeronautical mobile off-route service	normal	positions
1.35	aeronautical mobile-satellite service	normal	positions
1.36	aeronautical mobile-satellite route service	normal	positions
1.37	aeronautical mobile-satellite off-route service	normal	positions
1.38	broadcasting service	–	–
1.39	broadcasting satellite service	normal	positions

TABLE 1 (*end*)

ITU Radio Regulations		GGRF	
No.	**Service (Chapter I, Section III)**	**Dependency**	**Utilization**
1.40	radiodetermination service	–	–
1.41	radiodetermination-satellite service	high	positions
1.42	radionavigation service	normal	positions
1.43	radionavigation-satellite service	high	positions
1.44	maritime radionavigation service	normal	positions
1.45	maritime radionavigation-satellite service	high	positions
1.46	aeronautical radionavigation service	normal	positions
1.47	aeronautical radionavigation-satellite service	high	positions
1.48	radiolocation service	normal	positions
1.49	radiolocation-satellite service	high	positions
1.50	meteorological aids service	normal	positions
1.51	Earth exploration-satellite service	high	positions
1.52	meteorological-satellite service	high	positions
1.53	standard frequency and time signal service	normal	positions
1.54	standard frequency and time signal-satellite service	high	positions
1.55	space research service	high	positions
1.56	amateur service	normal	positions
1.57	amateur-satellite service	high	positions
1.58	radio astronomy service	high	positions

3 Operational overview of Geodetic VLBI measurements

For geodetic VLBI measurements, spatially separated radio telescopes simultaneously track the same extragalactic celestial object and receive its faint natural radio emission (see Fig. 4). The arrival times of the coherent wavefronts differ among the widely-spaced Earth-based telescopes by up to 0.02 second. This delay time τ is determined in a post-observation correlation process to a precision better than 100 picoseconds, if the radio telescope stations are equipped with stable frequency standards such as a hydrogen maser and compatible VLBI equipment.

When multiplied by the speed of light, each determined delay τ yields the distance between the radio telescopes in the direction toward the radio source. Observing more than three different sources gives the full three-dimensional separation between the radio telescopes, the so-called baseline.

A typical VLBI geodetic session involves 3 to 12 radio telescopes, lasts 24 hours, and utilizes hundreds to thousands of radio source observations with durations of 7 to 400 seconds (see Fig. 5). During a session, 50 to 100 different, nearly point-like radio sources are (repeatedly) observed. The observing schedule is optimized so that the sky distribution of observations at each station is as uniform as possible over all directions while maintaining contemporary visibility with as many telescopes in the network as possible. Sampling the variable atmospheric conditions rapidly and efficiently over the full sky is necessary in order to achieve the geodetic accuracy goals.

FIGURE 4

VLBI measurement principle and the processing chain

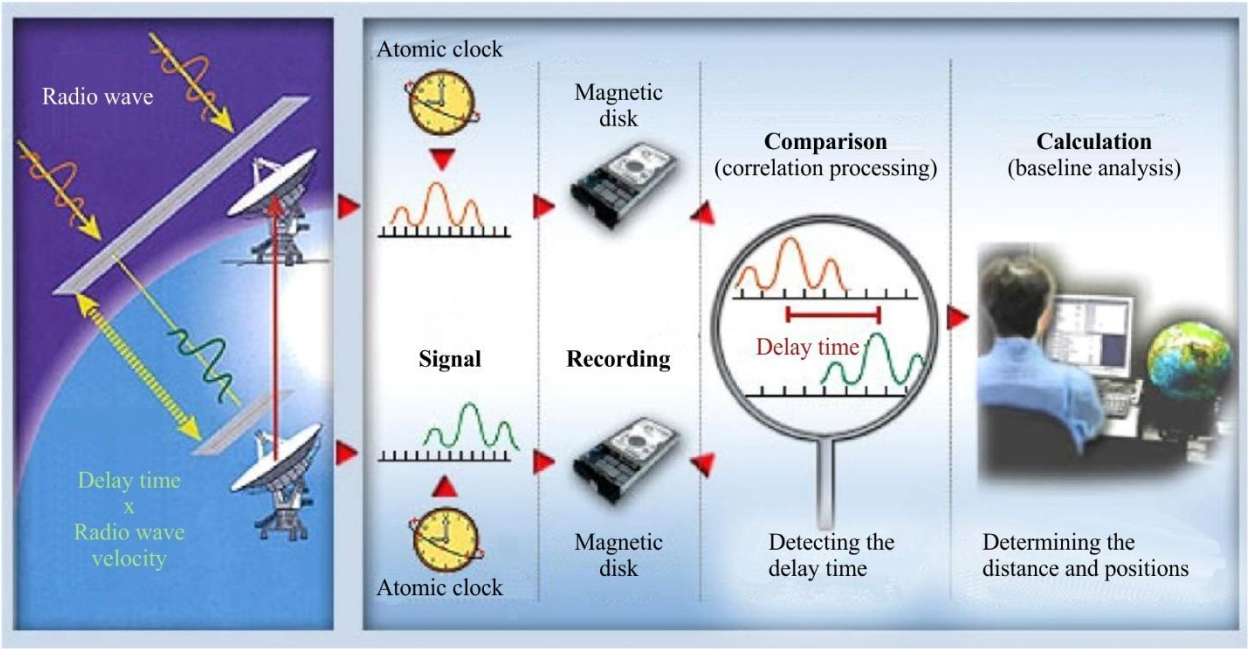

Note to Fig. 4: The delay time τ between the arrival time of coherent radio signals is measured/observed to determine radio telescope separation relative to the source. After the observations, the interferometer is formed by the cross-correlation of the digitised radio noise to determine the delay τ. Geodetic parameters are then estimated from the delay values from observations of many sources. (Figure from GSI Japan)

FIGURE 5

Typical set of VLBI scans at Westford, MA and Goddard, MD

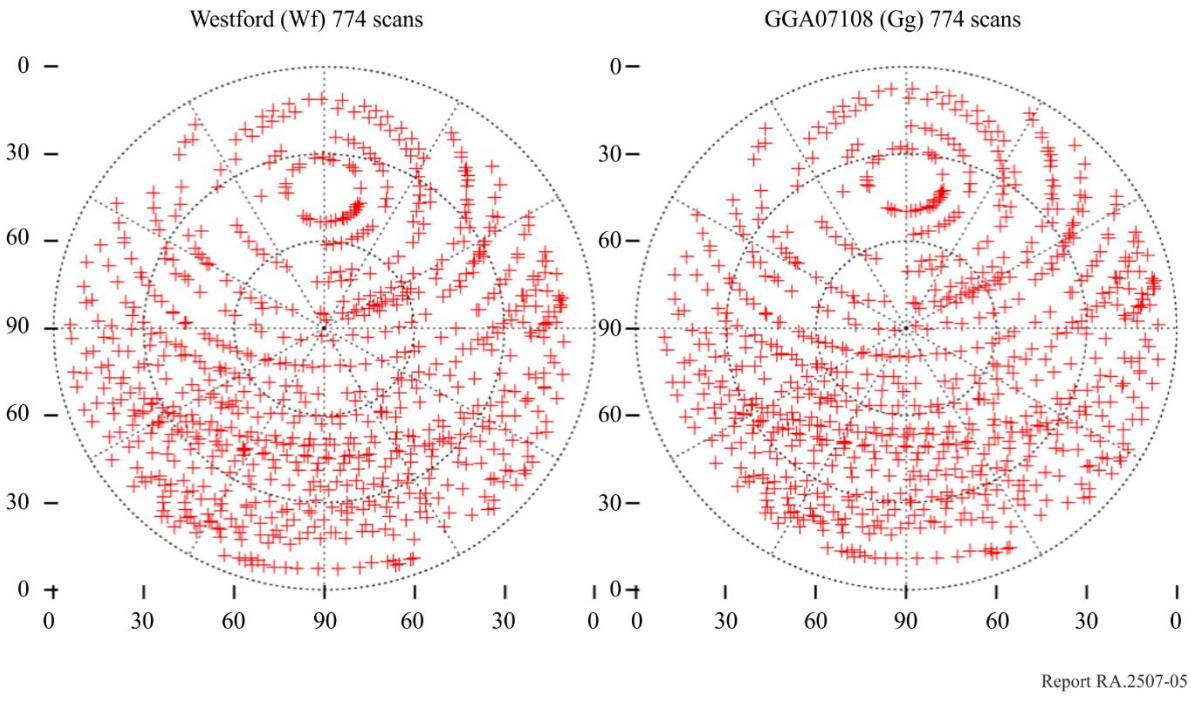

Note to Fig. 5: The observing mode involves multiple, short observations of faint radio sources at locations all over the sky. (Courtesy [3])

3.1 Frequency range

The legacy S/X-band geodetic VLBI system detects these signals in frequency ranges allocated for space-to-earth communications in S (2.20-2.38 GHz) and X (8.10-8.95 GHz) bands. The accuracy in the position on Earth obtained with the legacy system is at the centimetre level. This level falls short of the accuracy of 1 mm for position and of ±0.1 mm/yr for the rate targeted by GGOS. By the end of the 1990s the limitations of the legacy S/X had become evident, and the concept, originally called 'VLBI2010' and later renamed 'VLBI Global Observing System (VGOS)', was developed to replace the legacy geodetic VLBI system.

The plans for VGOS include a wideband receiver operating passively within the 2-14 GHz range in four blocks of up to 1 024 MHz bandwidth using eight channels each. The frequency bands allocated to the RAS which fall into the 2-14 GHz window are listed below (Table 2), including those bands with footnotes identifying their usage and encouraging administrations to take all practicable steps for the prevention of harmful interference (RR No. **5.149**).

TABLE 2

Frequency bands to be used by the RAS within 2-14 GHz with different protection levels: primary and secondary allocations and/or applicable provisions

Frequency (MHz)	Bandwidth (MHz)	Allocation, Footnote
2 655-2 670	15.0	secondary, No. **5.149**, **5.208B**
2 670-2 690	20.0	secondary, No. **5.149**, **5.208B**
2 690-2 700	10.0	PRIMARY, No. **5.340, 5.413, 5.208B**
3 260-3 270	7.0	No allocation, No. **5.149**
3 332-3 339	7.0	No allocation, No. **5.149**
3 345.8-3 352.5	6.7	No allocation, No. **5.149**
4 800-4 990	190.0	secondary, No. **5.149** applies in the 4 825-4 835 and 4 950-4 990 bands
4 990-5 000	10.0	PRIMARY, No. **5.149, 5.402, 5.443B**
6 650-6 675.2	25.2	No allocation, No. **5.149, 5.458A**
10 600-10 680	80.0	PRIMARY, No. **5.149**
10 680-10 700	20.0	PRIMARY, No. **5.340**

3.1.1 Frequency range motivation

Interferometric techniques have been used successfully over a wide range of the electromagnetic spectrum, with long standing success at radio frequencies. The following arguments narrow the preferred frequency bands for geodetic VLBI:

– Cosmic radio radiation from quasars or active galactic nuclei is weak. The radio spectral region with the lowest absorption by the Earth's atmosphere is approximately 1-18 GHz.

– The ionosphere delays a signal passing through it by a frequency-dependent amount that is in addition to the frequency-independent vacuum delay. At the frequencies of geodetic VLBI, the ionospheric delay is proportional to inverse frequency squared. By measuring the VLBI

delay of the quasar signal at multiple frequencies, the ionospheric delay can be determined and subtracted from the observed delay. The greater the ratio between highest and lowest observation frequency, the more precisely the ionospheric delay can be determined.

– The spanned bandwidth between lowest and highest observed frequency defines the precision of the delay measurement.

– Appropriate front-end and back-end hardware must be available at affordable cost.

Legacy S/X-band observations match the above considerations. Both bands are in the radio window. The ratio of nearly four between X- and S-band frequencies allows the ionospheric delay to be measured with high precision. VGOS observations rely on broadband feeds which had been developed recently for geodetic VLBI. The observation ranges from S-band (2.20-2.38 GHz) and X-band (8.10-8.95 GHz) have been extended upward to 14 GHz, covering much better the frequency range of the radio window and increasing the spanned bandwidth by a factor of 2 compared to legacy S/X.

The precision of the interferometric delay measurement and so for the geodetic results is proportional to the spanned frequency bandwidth on the radio source. Therefore, it is of interest to maximize the spanned bandwidth of the observed spectrum. But the recorded data rate and overall data volume are still limiting factors in geodetic VLBI. Hence, the frequency bandwidth synthesis technique using discrete observation channels with a total bandwidth much smaller than the overall highest-lowest frequency difference has been adopted to overcome this bottleneck.

Geodetic VLBI makes use of frequency bandwidth synthesis to maximize the precision with which observables are measured when constrained by limited recording bandwidth. The quality of a particular choice of frequency channels can be evaluated with the so-called delay resolution function. This function is constructed by first summing the cross-correlation products from all the frequency channels, where the phase of each product is the difference between the observed phase and a model phase given by RF frequency times a trial delay. The delay resolution function is the magnitude of this sum evaluated at many different trial delays. (Figure 14 presents examples of delay resolution functions created with simulated data.)

Determining the delay from a set of interferometric data then becomes a matter of searching over a range of trial delays to find the value at which the delay resolution function is maximized. If the combined frequency coverage of all the channels were to completely span the range from lowest to highest frequency, the function would have a single, sharp peak and very low ‘sidelobes’ around it, and the delay at the location of the peak would be the ‘true’ delay. With only a limited number of channels, however, the sidelobes can be much higher – nearly as high as the main peak if a poor choice is made for the channel frequencies – and the wrong delay peak may be selected, particularly when the SNR is low.

The ideal delay resolution function has a narrow main peak and low sidelobes. The quality of the function depends on the relative spacings of the frequency channels within the overall total bandwidth. Selecting the channel spacings based on a Golomb ruler[3], which delivers the maximum possible number of different spacings, gives the best results, but due to hardware constraints or other considerations, it is often not possible to strictly follow a Golomb ruler to assign all spacings. In that case an optimization procedure may be used to search over numerous sets of trial frequency assignments to find the best one.

In some cases, a Golomb ruler can be used for subsets of the channels without applying the ruler to all the channels. Once an optimum set of channel spacings has been determined, the entire set of

[3] In mathematics, a Golomb ruler is a set of marks at integer positions along a ruler such that no two pairs of marks are the same distance apart.

channels can be slid up or down in frequency while holding the spacings fixed. The choice of absolute channel frequencies can be influenced by factors such as how well the ionospheric delay can be estimated, how strongly the system sensitivity (SEFD) varies with frequency, and how many channels can be arranged to lie within protected RAS bands.

The geodetic astronomy spectrum is related to different observation targets. Legacy S/X-band observations were introduced in the 1980s using the technical components that were available at that time. The legacy S/X-band observations are still conducted in order to extend their unique, decades-long time series. Modern VGOS operations started with first trials in 2014 [3]. The aim is to reach 24 h/7 days VGOS operation. The introduction of VGOS broadband receivers covering the range of 2-14 GHz enabled the expansion of the legacy S/X-band capabilities and enhanced the spanned bandwidth, which is one condition to provide mm accuracy for the GGRF.

S/X/Ka observations are less frequent and are used basically to tie the legacy time series to new VGOS telescopes during a transition period and/or to improve the X/Ka CRF, which is important for deep space missions. Table 3 gives an overview of the observed frequency ranges.

TABLE 3

Mode	Frequencies (GHz)	Since
Legacy S/X	2.20-2.39 8.20-8.95	1979
S/X/Ka	2.20-2.70 7.50-9.00 28.00-33.00	2014
VGOS	2.00-14.00	2015

3.2 Legacy and planned systems

The VGOS concept includes 40 globally distributed observatories. Existing and planned sites are denoted in Fig. 6.

FIGURE 6

The global VGOS-network with existing VGOS stations and planned VGOS sites (as of 2021)

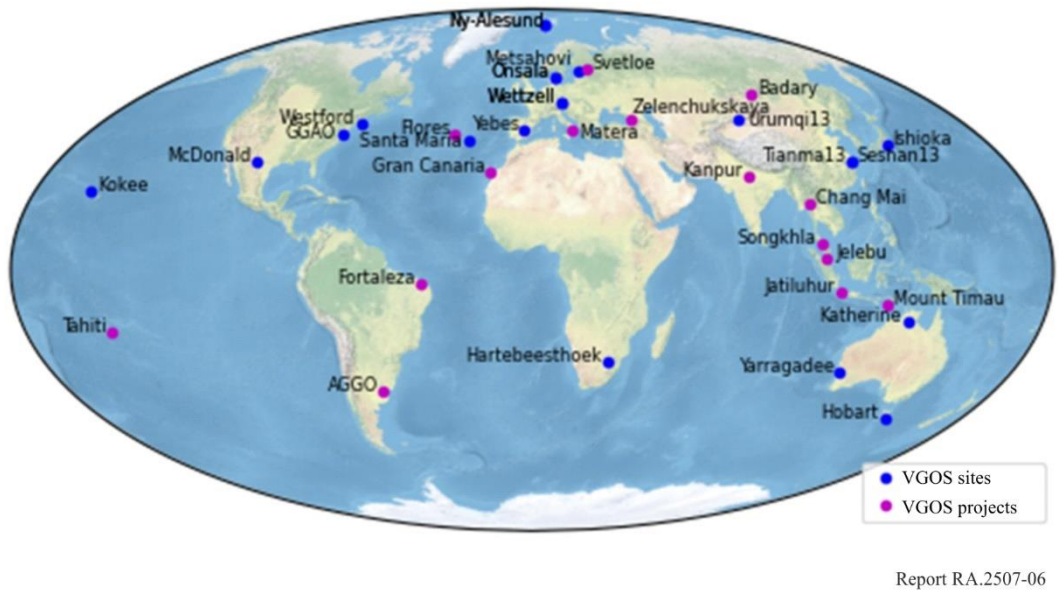

To achieve all VGOS defined goals, a global VLBI network of similar radio telescopes is being created for the first time. Ideally this global network would consist of evenly distributed sites, each meeting the same technical specifications. Due to the uneven distributions of landmass and oceans, existing telescopes are unevenly distributed over the globe. Achieving a more uniform distribution entails building VGOS stations at new locations.

The most important technical characteristics of a VGOS site are:

1) the use of a cooled broadband receiver which can observe simultaneously selectable bands in the range of 2 to 14 GHz, and

2) an antenna with a reflector diameter $\gtrsim$12 m that can slew in azimuth at 12 degrees/s and in elevation at 6 degrees/s.

VGOS aims at continuous operation of 24 hours for 7 days a week, which can best be met by redundant radio telescopes at the same site. This requirement leads to the twin telescope concept. The global expansion of the radio telescopes of VGOS depends on national efforts which in turn depend upon voluntary commitments and the capabilities of the individual institutions.

The accuracy of VGOS measurements depends on signal-to-noise achieved with each observation. Due to weak natural astronomical sources, increased bandwidth leads to better observational data. For VGOS, currently each of four frequency ranges of operation (blocks) within 2-14 GHz (including bands allocated to the RAS with some protections and bands where no protection can be claimed) covers up to 1 024 MHz bandwidth and contains a minimum of eight channels, each 32 to 128 MHz wide. Ideally, at least three spatially separated telescopes observe the same source simultaneously. The incoming signal at each radio telescope is digitized, tagged with arrival time stamps, and recorded. The coherent cosmic radiation is detected in the correlation process after the observation. The primary interferometric outputs from the correlation process used in astrometry and geodesy are the fringe phase and its frequency derivative, group delay.

The new VGOS system will improve geodetic accuracy by using fast-slewing antennas with primary reflectors of diameter 12 to 13 m and a broadband signal acquisition chain (2-14 GHz) with fast-sampling digital electronics.

As the antennas used for VLBI are highly directional, usually only one source can be observed at a time. Between observations, the antenna moves on to the next source. The fast-slewing antennas ensure a decrease in the source-switching interval and a resulting increase in the number of observations per unit time. Compared with legacy observations, VGOS observations thus have a higher temporal and spatial resolution, which will contribute to reducing errors in the geodetic results, most notably errors resulting from spatial and temporal variations in the atmospheric water vapour content, which affects the delay of the radio signal as it passes through the atmosphere.

The broadband signal acquisition chain employed in VGOS allows for shorter on-source observing time while maintaining the same delay precision. Currently, four widely spaced frequency bands are selected from the 2-14 GHz range. By using a technique known as bandwidth synthesis [5], the total span, from lowest to highest frequency, of the four bands defines the delay measurement precision per unit time. Being able to select the band frequencies allows for frequencies most RFI-free to be used thus reducing increasingly prevalent issues with RFI. However, the use of parts of the 2-14 GHz band by new transmitting radio services will limit the opportunistic ability for VGOS observations. A frequency channel impacted by signals at one site will be lost on all the baselines to that station.

Table 4 gives an overview of the global distribution of operational and planned VGOS sites (as of June 2021).

TABLE 4

Existing and planned VGOS global radio telescope network

ITU-Region	Country	Location	N Latitude (° ‘ “)	E Longitude (° ‘ “)	Reflector size (m)
R1	Finland	Metsähovi	60 13 04.8	24 23 38.4	13.2
R1	Germany	Wettzell North	49 08 38.1	12 52 39.4	13.2
R1	Germany	Wettzell South	49 08 36.4	12 52 41.6	13.2
R1	Italy	Matera (planned)	40 38 56.4	16 42 18.0	13.2 (?)
R1	Norway	Ny Alesund North	78 56 36.1	11 51 17.1	13.2
R1	Norway	Ny Alesund South	78 56 33.4	11 51 19.5	13.2
R1	Portugal	Flores (planned)	39 22 34.0	-31 11 42.0	13.2
R1	Portugal	Santa Maria	36 59 06.0	-25 07 33.6	13.2
R1	Russia	Badary (planned)	51 46 12.0	102 14 02.4	13.2
R1	Russia	Svetloe (planned)	60 31 48.0	29 46 48.0	13.2
R1	Russia	Zelenchukskaya (planned)	43 47 16.8	41 33 54.0	13.2
R1	South Africa	Hartebeesthoek	-25 53 16.8	27 41 09.6	13.2
R1	Spain	Gran Canaria (planned)	27 53 58.4	-15 30 28.6	13.2
R1	Spain	Yebes	40 31 22.8	-03 05 16.8	13.2
R1	Sweden	Onsala NE	57 23 38.4	11 55 12.0	13.2
R1	Sweden	Onsala SW	57 23 34.8	11 55 08.4	13.2
R2	Argentina	AGGO (planned)	-34 52 21.4	-58 08 23.2	13.2 (?)
R2	Brazil	Fortaleza (planned)	-03 52 41.6	-38 25 31.4	12.0 (?)
R2	USA	GGAO	39 01 19.2	-76 49 38.3	12.0
R2	USA	Kokee Park	22 07 35.3	-159 39 53.9	12.0

TABLE 4 *(end)*

ITU-Region	Country	Location	N Latitude (° ‘ “)	E Longitude (° ‘ “)	Reflector size (m)
R2	USA	McDonald	30 40 49.4	-104 01 25.1	12.0
R2	USA	Westford	42 36 46.8	-71 29 37.7	18.3
R3	Australia	Hobart	-42 36 46.8	147 26 16.8	12.0
R3	Australia	Katherine	-14 22 30.0	132 09 07.2	12.0
R3	Australia	Yarragadee	-29 02 49.2	115 20 45.6	12.0
R3	China	Seshan	31 05 58.4	121 11 57.6	13.0
R3	China	Tianma	31 05 26.3	121 08 12.3	13.2
R3	China	Urumqi	43 28 20.1	87 10 25.1	13.0
R3	Japan	Ishioka	36 06 10.8	140 05 20.4	13.2
R3	France	Tahiti (planned)	-17 39 03.1	-149 25 33.5	12.0 (?)
R3	India	Kanpur (planned)	26 31 09.3	80 13 55.2	13.2
R3	Indonesia	Jatiluhur (planned)	-06 31 16.5	107 24 39.4	18.3
R3	Malaysia	Jelebu (planned)	03 03 10.8	102 03 50.4	13.0
R3	Thailand	Chiang Mai (planned)	18 51 56.0	99 13 03.4	13.0
R3	Thailand	Songkhla (planned)	07 09 23.7	100 36 48.0	13.2

4 Technical details of geodetic VLBI

A geodetic VLBI network station is composed of the following components:

– a radio telescope with large efficient reflector to focus faint cosmic radiation;

– a suitable feed to observe a large bandwidth on the radio source to maximize signal detection sensitivity and minimize delay measurement uncertainty;

– a low noise receiving system (see Fig. 7);

– a digitizing system with high sampling rate;

– a high-speed recording system;

– a high-data-rate transport system to transfer data from the station to the correlator;

– a hydrogen maser as local reference oscillator to serve as high-stability time and frequency standard for all the VLBI electronics;

– a phase calibration system to measure frequency and temporal variations in instrumental phases and delays, in order to allow for the correlated VLBI data to be corrected for their effects;

– a cable delay measurement system to allow correction for temporal delay variations in the cable carrying the phase calibration reference signal to the front-end.

FIGURE 7

Typical VGOS 2.2-14 GHz broadband cryogenic receiver signal chain at a NASA station

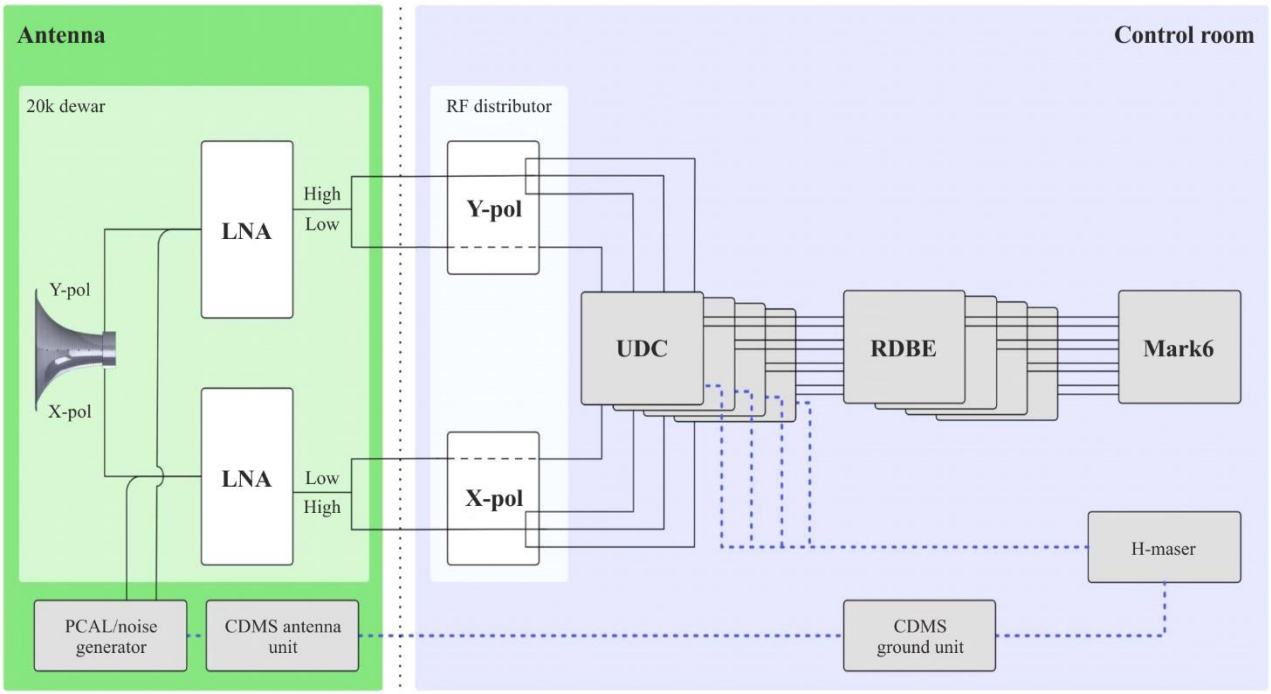

LNA: Low Noise Amplifier; UDC: Up-Down Converter; RDBE: Reconfigurable Digital Back End; Mark6: Recorder; PCAL: Phase Cal (CDMS) Cable Delay Measurement System [3]

4.1 VGOS radio telescopes

Simulations showed that VGOS goals could be reached only by increasing the number of observations per time unit. Instead of making 200 to 400 observations per site over 24h, as is typical with legacy systems, the VGOS observation scheme relies on on-source observation time of order 10 s plus 20 s slewing time, resulting in around 3000 observations within 24 h. This observation mode can only be executed with very agile and robust radio telescopes. To reach any source in the sky within 20 s requires kinematic parameters of 12 degrees/s speed for azimuth and 6 degrees/s for elevation. The maximum acceleration might be as high as 3 degrees/s^2. The determination of the reflector size for VGOS depends on:

– the mass used in the construction for the moving parts to move quickly (less is better);

– the stiffness of the reflector to resist deforming forces (gravity, wind, slewing) (the higher the better, however it does increase mass for rigidity);

– the desired signal to noise ratio, which depends on collecting area (the larger the better, however it does increase the mass due to larger diameter).

FIGURE 8

The VGOS radio telescopes at the Geodetic Observatory Wettzell, Germany

Report RA.2507-08

Note to Fig. 8: The Twin Telescope Wettzell (TTW) has been the first rigorous VGOS telescope construction (inaugurated in 2013).

Studies in the early stages of VGOS development led to the conclusion that the best compromise among these contradictory factors was a diameter of ~12-15 m. Two different VGOS radio telescope styles are shown in the accompanying figures: shaped reflector in Fig. 9 (left); ring-focus telescopes in Fig. 9 (right). Both VGOS and legacy S/X observations rely heavily on KPGO for its unique position on the Earth. The solid construction of the static part (base or pedestal) makes the radio telescope a geodetic monument and provides a stable reference over decadal periods. The presence of twin telescopes as at Wettzell in Fig. 8 allows for continuous observations, independent of maintenance periods, and for the application of new observation strategies when the telescopes are used in parallel. The VGOS operational system characteristics are designed for broadband operation of the receiver from 2 to 14 GHz. Different broadband feed designs have been developed for VGOS. These broadband feeds have different polarisation properties (dual linear or circular) and different types of output interfaces (single-ended or differential) to the low noise amplifier (LNA). However, all of them have a broad beamwidth and low gain, which means the reflector optics must have a small f/D of ~0.3. In a dual reflector radio telescope, it is unusual to have such a low f/D due to the fact that it can lead to a large blockage area. The ring-focus design, however, avoids much of the blockage both from the feed and the sub-reflector when a feed with low f/D is used (see Fig. 10).

FIGURE 9

Radio telescopes used for geodetic VLBI

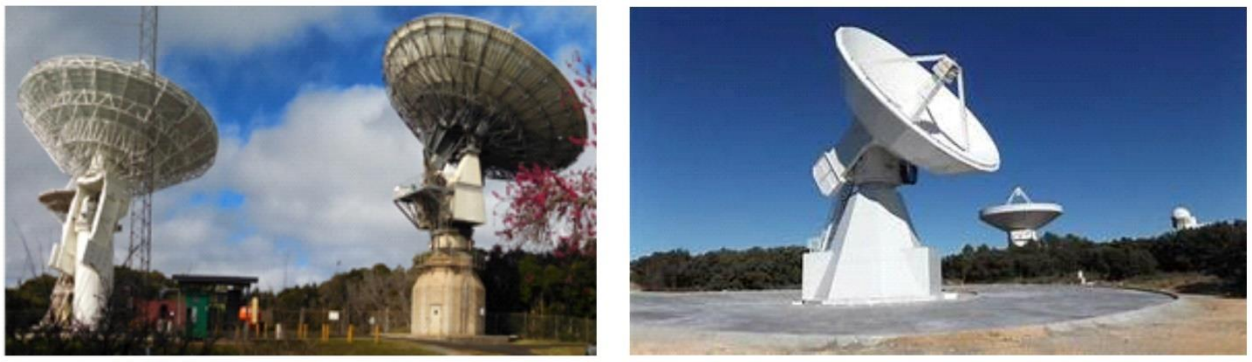

Report RA.2507-09

12 m shaped reflector VGOS antenna at Koke'e Park Geophysical Observatory beside the older 20 m reflector used for S/X observations

RAEGE[4] 13.2 m radio telescopes at Yebes (Spain)

Note to Fig. 9: Radio Telescopes Used for Geodetic VLBI, where Rho is the distance from the rotational axis z to create the parabolic reflector. (Left) 12 m shaped reflector VGOS antenna (left) at Koke'e Park Geophysical Observatory beside the older 20 m reflector used for S/X observations (Right) RAEGE[4]13.2 m radio telescopes at Yebes (Spain). It is the same type used at Santa María (Açores, Portugal), which are compliant with VGOS specifications. The future RAEGE radio telescopes at Gran Canaria and Flores Island (Açores) will also follow this design.

FIGURE 10

Example of VGOS ring-focus design for the VGOS RAEGE radio telescope reflector profile

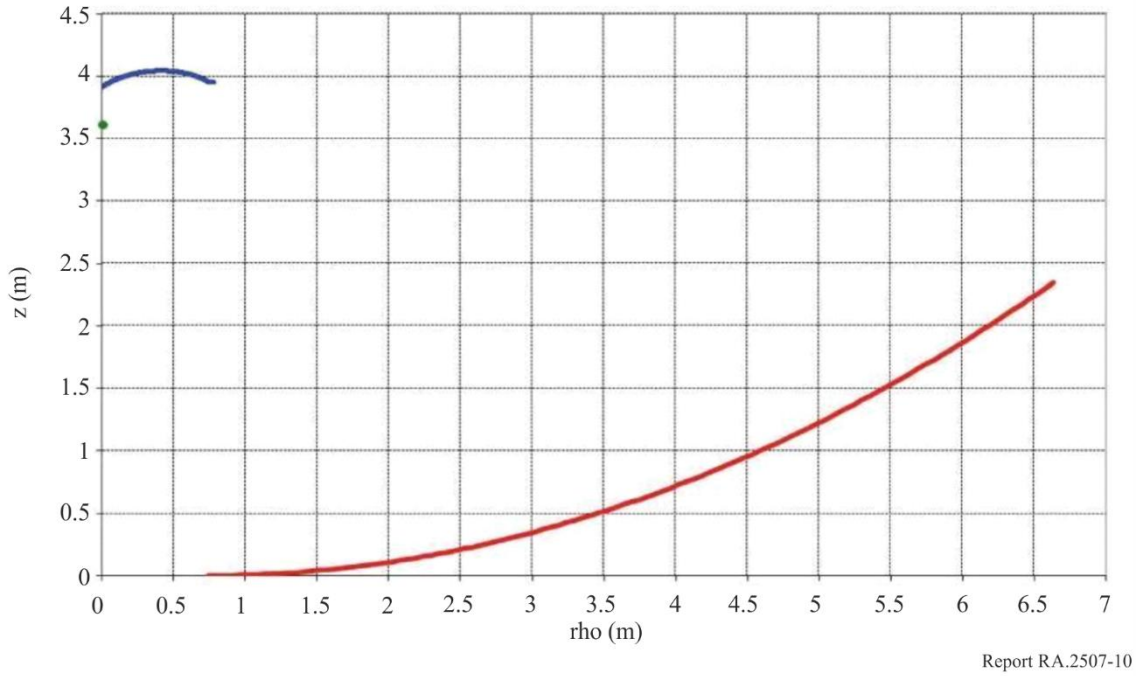

Report RA.2507-10

[4] RAEGE: Red Atlántica de Estaciones Geodinámicas y Espaciales, Spanish-Portuguese VLBI-network (www.raege.eu)

Note to Fig. 10: The red curve is the parabola defining (when rotated around the z-axis) the main reflector, the blue line indicates the shape of the secondary reflector, and the green dot marks the focal point of the ring-focus system, where the receiving feed needs to be placed.

Some of the new VGOS radio telescope infrastructure will replace older radio telescopes when they retire. For continuity of the geodetic time series of the reference points the new installation has to be in the vicinity to the former one. Furthermore, common observations with both radio telescopes (VGOS and legacy systems) should also be carried out for a period of time in order to establish a good link between the two different reference points. New geodetic VLBI sites will be selected only in regions where no geodetic observatory exists. New sites must meet suitable conditions. The avoidance of interference is one important criterion and is as important as, for example, geological site stability.

4.2 Wideband receivers

In geodetic VLBI the wideband feed needs to have a frequency-independent phase centre location and high polarization purity. These properties have been met at first with dual linear polarized feeds. Several different wideband feed designs have been prototyped for VLBI. Currently, the QRFH-feed design is a prominent component at VGOS network stations (Table 5, Figs 11 and 12), because it allows for easy phase calibration injection in front of the first low-noise amplifier, unlike some designs that require differential-input low-noise amplifiers.

TABLE 5

Technical parameters for a combined ARCH feed and low-noise amplifier used for the VLBI Global Observing System

QRFH parameter	Value
Frequency range (GHz)	2-14
Noise temperature (K)	< 20
Gain (dB)	60
Gain flatness (dBpp)	4
Output return loss (dB)	14
Pout 1 dB (dBm)	+14
Cooldown time (hours)	3
Antenna efficiency (%)	up to 60%
Axial cross-polar isolation (dB)	>15

FIGURE 11

Schematic view of the QRFH feed and its dewar

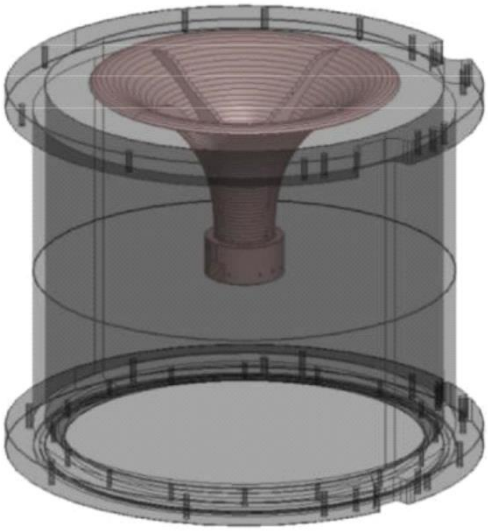

Report RA.2507-11

Note to Fig. 11: Wideband feeds provide small gain and are together with the first amplifiers exposed to a cryogenically cooled environment. The dewar is evacuated and serves as an isolator against the 300 K environment.

FIGURE 12

Schematic view of the feed conus at the radio telescope

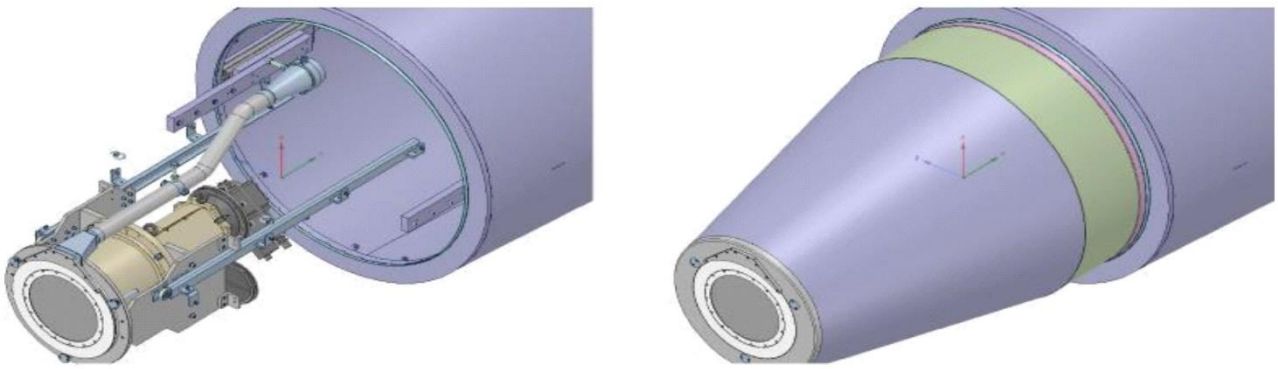

Report RA.2507-12

Note to Fig. 12: For maintenance and receiver change, the feed conus must be dismountable. Due to the lack of space and the heavy component a rail system supports the disassembling procedure. The feed blowing system prevents icing at the Rexolite® front disk.

The signal processing at the front end differs from the S/X-band as the two linear polarizations, vertical and horizontal, need to be treated in two separated signal paths in order to combine these to a circular polarization in the correlation process.

4.3 Calibration systems

The phase, cable delay and amplitude calibration systems provide fundamental calibration signals for the geodetic VLBI observations.

4.3.1 Phase calibration

As the radio signal from the quasar passes through the front-end and back-end electronics, it undergoes time- and frequency-dependent phase changes caused by the instrumentation. To ensure the highest data quality, these instrumental phase and delay effects must be removed from the data. The standard correction method makes use of a stable, broadband 'phase calibration' signal injected via a directional coupler between the feed and LNA. In its passage through the signal chain, it is subjected to the same instrumental effects as is the quasar signal. The calibration signal detected in the recorded data can then be used to subtract the instrumental effects from the incoming quasar signal. The Phasecal Antenna Unit (AU), located close to the receiver feed, generates the calibration signal, which viewed in the time domain is a pulse train and in the frequency domain is a series of equally spaced tones extending over the 2-14 GHz range. The spacing between tones is typically 5 MHz, which corresponds to a pulse period of 200 ns. The pulse generator in the AU is driven by a reference signal – usually a 5 MHz tone – from the hydrogen maser. All the circuitry of the AU is inside a temperature-stabilised enclosure designed to attenuate RFI leakage (see Fig. 13).

The temperature is stabilised through a Peltier thermo-electric cooler. As a result, the instrumental phase changes can be measured at 5 MHz steps across the band, as the correlator extracts both amplitude and phase for each tone. However, an ambiguity of 200 ns is present due to the 5 MHz spacing.

FIGURE 13

Phasecal AU developed by Yebes Observatory (Spain)

Report RA.2507-13

4.3.2 Cable delay measurement system

The phase calibration method can work properly only if the phase of the reference signal driving the AU pulse generator is stable, or if any variations in that phase are measured and applied as corrections to the tone phases in the recorded data. Because the cable carrying the reference signal from the maser to the AU is inevitably subject to temperature variations and cable flexure, which in turn affect the signal phase, the latter option has been adopted in geodetic VLBI systems. A so-called Cable Delay Measurement System (CDMS) is employed to monitor temporal delay variations in the cable at the

reference frequency. This measurement must be done with picosecond precision to reach the VGOS goal of 1 mm accuracy in position determination.

4.3.3 Amplitude calibration system

In common with most radio astronomical receivers, geodetic VLBI receivers also include an amplitude, or noise, calibration system to monitor system temperature. The noise calibration signal is white Gaussian noise that is injected, together with the phase calibration signal, between the feed and LNAs. It is typically cycled on and off at an 80 Hz rate with a 50% duty cycle and is synchronously detected in the back-end. In order to allow continuous monitoring without appreciably increasing the system temperature, the noise calibration signal is set to no more than ~5% of the system temperature.

4.4 Data acquisition systems (DBBC2, −3, Flexbuff, Mk6)

The main back-end system is the Digital Baseband Converter (DBBC) (Fig. 11), replacing the analogue baseband converters. DBBCs digitize analogue signals at sampling rates 512, 1 024 or 2 048 MHz. The DBBC is equipped with FILA-units. FILA-unit converts VLBI Standard Interface (VSI) data stream to the VLBI Data Interface Format (VDIF). VDIF data can be streamed with several Gbit/s in total through two optical ports equipped with XFP transceivers. New generations of DBBC3 and DBBC4 providing higher data rates have been developed by HatLab company, Italy. Alternative developments are the Japanese ADS-3000+ sampler (Fig. 14) or the US development DBE. Currently, the most used recording system is FlexBuff. FlexBuffs are computers equipped with many SAS (Serial Attached SCSI) disks with a total capacity of several hundreds of terabytes (TB). FlexBuffs are based on commercially available off-the-shelf (COTS) components and run under open software. Also, the latest version of Mark-generations, Mark6, is in use.

FIGURE 14

Left: The DBBC2 and DBBC3. Right: The DBBC2 and the ADS3000+

Report RA.2507-14

4.5 Reference frequency and timing

As mentioned above, geodetic VLBI is the only space geodesy technique capable of measuring the Earth rotation phase, or time UT1, with respect to the Celestial Reference Frame. This time is related with civil time with the help of a GNSS clock at each VLBI station. The recorded VLBI data are time-tagged using the time information from the GNSS clock. In this manner, the time difference UT1-UTC can be determined.

Most important for frequency and time accuracy in a VGOS system is a reference frequency oscillator that is highly stable both on short time scales, for phase-locking various oscillators in the VLBI signal chain, and on long time scales, for providing a stable time base to ensure signal coherence between widely separated VLBI stations. This requirement is fulfilled by commercially available hydrogen masers.

4.6 Infrastructural requirements

VGOS sites are typically connected by optical fibre links to broadband communication networks. VLBI data cannot be compressed as the content is white noise from the quasar as well as from the environment and electronics. Therefore, the raw data volume of up to 100 TB per 24 hours acquired at the globally distributed radio telescope sites has to be brought together at one correlation centre for correlation at a later time. For the full VGOS deployment, 10 Gbit/s fibre links will be required.

For continuous operation a stable electric energy supply is a requirement. The site should be equipped with an energy backup system providing 24/7 service. Additionally, an accurate weather station is required, as weather data are needed for accurate computation of atmospheric refraction, needed for accurate pointing of the telescope, and delay, needed at the data analysis stage.

4.7 VGOS frequency setup

The broadband feed is a new feature for geodetic astronomy as it allows observing over a wider frequency range, with corresponding improvement in delay precision, and it allows more flexibility in finding the optimized frequency configuration with respect to the observing network. In general, the full spectral range of the receiver is subject for mitigation to avoid amplifier saturation, which will degrade the sensitivity over the full amplifier bandwidth and not just in the spectral regions where terrestrial radio noise is present. Because only specific frequency channels are observed within the range of 2-14 GHz, they are most in need of mitigation. Most VGOS observations since 2015 have used the frequency configuration VGOS-480 (Table 6). This setup makes use of four frequency blocks A, B, C, D, each with a spanned bandwidth of 480 MHz. Each block contains eight 32-MHz-wide channels distributed with spacings of integer multiples of 32 MHz.

As described above an efficient configuration of the observation channels can be found with the optimization of the delay resolution function. The VGOS broadband receiver capabilities and the back-end hardware are a flexible system which may be used for numerous different setups. To improve geodetic VLBI precision, other configurations have been devised. One configuration setup is VGOS-992 (Table 6), but also other setups that include Ku band and/or make rigorous use of the Golomb ruler to create better delay resolution functions are under investigation. An example sequence $\underline{G}(8)^1(-2)$ is given in Table 6 and the simulated comparison of these three sequences is shown in Fig. 15. In VGOS, the geometric group delay and ionospheric total electron content difference between the two stations of a baseline are estimated simultaneously by fitting a frequency model to the channel fringe phases. These two parameter estimates are highly correlated, and an additional consideration in choosing a frequency sequence, which was alluded to in § 3.1, is the intent to reduce the degree of correlation and hence to improve the delay precision. New frequency sequences to be observed are very much dependent on the technical capabilities of the VLBI hardware at the stations. Further optimization may take place in the future.

The VGOS frequency setup is structured in four frequency blocks (A, B, C, D) with 8 associated channels. Each channel has a bandwidth of 32 MHz. The VGOS-480 setup has been used for commissioning of new VGOS radio telescopes and is also called 'VGOS Demonstration Series' (VDS). VGOS-992 is based on the same bands as for VGOS-480, but the eight channels cover 992 MHz bandwidth. The G(8)1(-2) is using a sequence based on Golomb order 8 and extending to the Ku-band. It is a possible example for the future evolution of VGOS. The listed frequencies are lower side-band and refer to the lower frequency edge of the channel. Add 32 MHz for the value of the high frequency edge; e.g. start: 3 000.4 MHz, end: 3 000.4 MHz + 32 MHz = 3 032.4 MHz. These channels are recorded for horizontal and vertical linear polarization, 64 channels in total. See Table 6.

TABLE 6

Setup	**VGOS-480**	**VGOS-992**	**G(8)[1](-2)**
Spanned bandwidth per band (MHz)	480	992	992
Polarization	H, V	H, V	H,V
Channel bandwidth (MHz)	32	32	32
Block A, start frequencies (MHz)			
A1	3 000.4	3 000.4	3 000.4
A2	3 032.4	3 032.4	3 032.4
A3	3 064.4	3 128.4	3 128.4
A4	3 192.4	3 288.4	3 288.4
A5	3 288.4	3 576.4	3 480.4
A6	3 352.4	3 768.4	3 704.4
A7	3 416.4	3 896.4	3 928.4
A8	3 448.4	3 960.4	3 960.4
Block B, start frequencies (MHz)			
B1	5 240.4	5 240.4	5 304.4
B2	5 272.4	5 272.4	5 336.4
B3	5 304.4	5 368.4	5 432.4
B4	5 432.4	5 528.4	5 592.4
B5	5 528.4	5 816.4	5 784.4
B6	5 592.4	6 008.4	6 008.4
B7	5 656.4	6 136.4	6 232.4
B8	5 688.4	6 200.4	6 264.4
Block C, start frequencies (MHz)			
C1	6 360.4	6 360.4	7 864.4
C2	6 392.4	6 392.4	7 896.4
C3	6 424.4	6 488.4	7 992.4
C4	6 552.4	6 648.4	8 152.4
C5	6 648.4	6 936.4	8 344.4
C6	6 712.4	7 128.4	8 568.4
C7	6 776.4	7 256.4	8 792.4

TABLE 6 (*end*)

Setup	VGOS-480	VGOS-992	G(8)[1](-2)
C8	6 808.4	7 320.4	8 824.4
Block D, start frequencies (MHz)			
D1	10 200.4	10 200.4	12 888.4
D2	10 232.4	10 232.4	12 920.4
D3	10 264.4	10 328.4	13 016.4
D4	10 392.4	10 488.4	13 176.4
D5	10 488.4	10 776.4	13 368.4
D6	10 552.4	10 968.4	13 592.4
D7	10 616.4	11 096.4	13 816.4
D8	10 648.4	11 160.4	13 848.4
Number of recorded channels	64	64	64
Total bit rate (Mbit/s)	8 192	8 192	8 192
Accumulated channel bandwidth (MHz)	1 024	1 024	1 024

FIGURE 15

Comparison of delay resolution functions for three possible VGOS frequency sequences (Table 6)

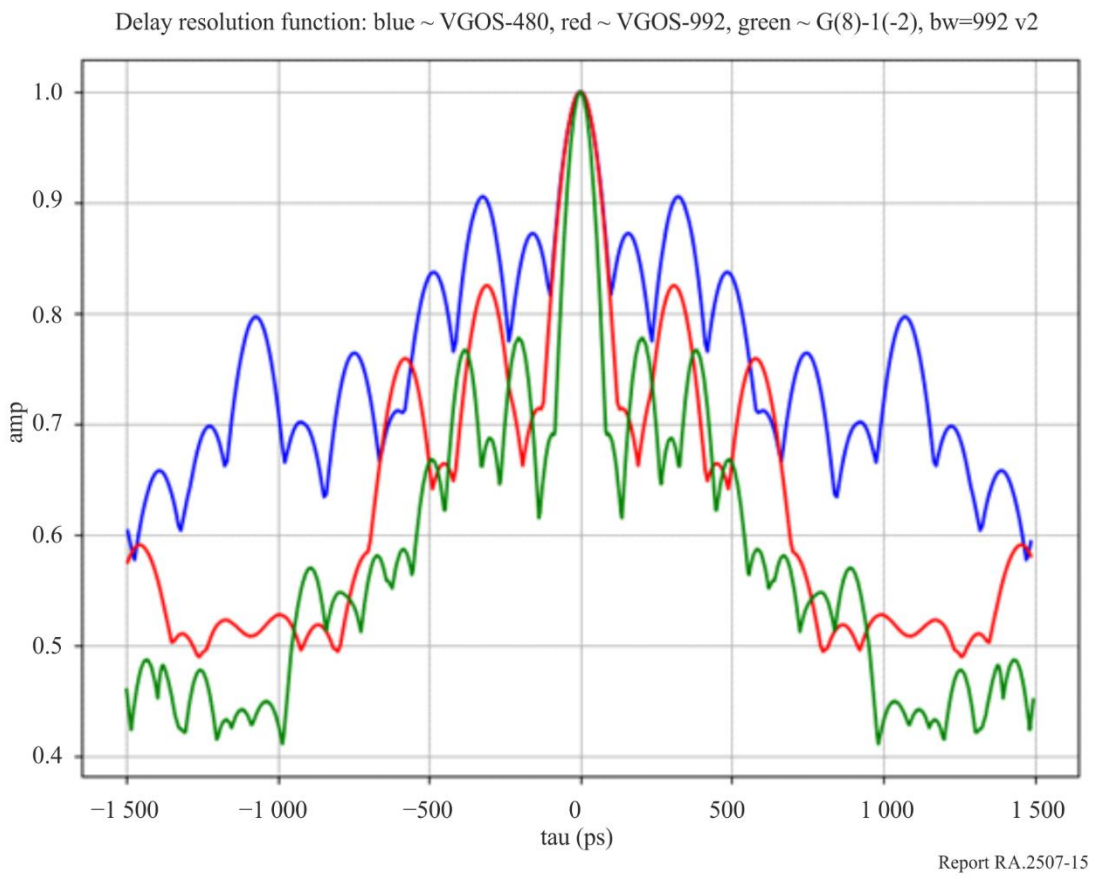

Note to Fig. 15: The quality is indicated by the width of the main peak (the narrower the better) and the height of the sidelobes (the lower the better, to reduce the likelihood the delay estimation process will select the wrong

peak in the presence of noise). The frequency span of each band in sequence VGOS-992 is twice that in VGOS-480, hence the channels can be spread more nearly uniformly over 3-11 GHz, with a resulting improvement in sidelobe levels. The inclusion of Ku-band in $G(8)^1(-2)$ provides further improvement, both in sidelobe level and in main peak width.

5 Strategies to maximize system performance

Unwanted radio noise in VGOS system receivers causes loss of accuracy in geodetic and astrometric measurements and can be partly addressed by the following: operational work-around, engineering techniques, and smart technologies.

Operations

– Site VGOS stations in existing radio quiet zones or coordination zones where additional domestic regulatory protections may exist for radio astronomy or geodetic observations.

– Adjust the horizon mask to exclude terrestrial transmitters. Masking will decrease access to astronomical radio sources at low elevation angles, which occur naturally when telescopes are widely separated and which are needed for better atmospheric sampling. Excluding low-elevation zones decreases the high-accuracy potential of VGOS.

– Adapt the scheduling procedures used to sequence individual VLBI observations to be able to account for the predictable presence of detrimental spaceborne emissions. The predicted impact may range from minor degradation of performance to damaging the VLBI equipment. Adapt the scheduling procedures to observe the source at a particular time when the level of degradation is acceptable for each antenna.

Engineering

– Make use of filters at the receiver's front end. Radio telescope stations are developing different filters to attenuate RFI at the front end, to avoid the saturation or destruction of the low noise amplifier. With 32 observation channels it will be quite difficult to implement a filter system which rejects all interference. Bandpass and notch filters as RFI blockers are being investigated. To prevent saturation of the low-noise amplifiers, which are normally cooled cryogenically, filters must be placed between the feed and amplifier. Presently only high-temperature superconductor (HTS) filters, which are quite expensive to implement, have the requisite performance. In order to avoid RFI-generated intermodulation signals in the observing bands, some stations are required to introduce high-pass filters in their signal chain to cut off RFI below 3 GHz. This means a reduction in the operating frequency range of VGOS from 2-14 GHz and, if the filter is placed between the feed and LNA, extra cost and complexity in receiver development, as well as a slight degradation of receiver sensitivity.

– Make use of filters at the back end. Some mitigation can be applied after digitization using digital filters, providing that the receiver signal chain is not saturated by RFI. This subject needs investigation and technical development.

Smart technology

– Software mitigation, providing that there is no saturation in the receiver signal chain. This software claims to estimate and subtract radio noise in radio astronomical observations off-line [6], [7], [8]. However, this technique needs more current research in geodetic VLBI applications.

5.1 Calculation of levels detrimental to achieve VGOS goals

Levels of interference detrimental to VGOS are approximately the same as what can be found in Recommendation ITU-R RA.769. In this section, we provide calculations using the parameters of VGOS operations to demonstrate that approximately the same levels are needed.

To determine the interference levels detrimental to VGOS operations, two different scenarios have to be considered. Firstly, the calibration process of the radio telescope that is carried out in single dish (continuum) mode, and secondly the geodetic observation which is performed as a VLBI interferometer.

The calibration is regularly done before and after a 24 h VLBI-session for the system checkout during 1 h and occasionally for pointing modelling during up to 24 h. During a 24 h VLBI session each source scan is tagged with a system temperature measurement up to every 30 s (2880 times/24 h).

Following the procedure in the Recommendation ITU-R RA.769, threshold levels for detrimental interferences in the frequency range of VGOS receivers (2-14 GHz) are computed in this section for both scenarios.

On the one hand, the computation of the continuum mode scenario follows the same approach and considerations as provided in Recommendation ITU-R RA.769. However, the typical integration time in VGOS during calibration is 100 s, so this value has been considered in the computations instead of the value of 2000 s applied in Recommendation ITU-R RA.769. The results are shown in this report (Annex), where the specific threshold levels for calibration in the single-dish continuum mode in the frequency range of VGOS (2-14 GHz), as split into 32 MHz channels, are given.

According to Annex 1 in Recommendation ITU-R RA.769, the sensitivity of an observation in radio astronomy can be defined in terms of the smallest power level change ΔP in the power level P at the radiometer input that can be detected and measured. The sensitivity equation is:

$$\frac{\Delta P}{P} = \frac{1}{\sqrt{\Delta f_0 t}} \tag{1}$$

where:

P and ΔP : power spectral density of the noise

Δf_0 : bandwidth

t : integration time. P and ΔP in equation (1) can be expressed in temperature units through the Boltzmann's constant, k:

$$\Delta P = k\,\Delta T; \qquad \text{also} \qquad P = kT \tag{2}$$

Thus the sensitivity equation may be expressed as:

$$\Delta T = \frac{T}{\sqrt{\Delta f_0 t}} \tag{3}$$

where:

$$T = T_A + T_R$$

This result applies for one polarization of the radio telescope. T is the sum of T_A (the antenna noise temperature contribution from the cosmic background, the Earth's atmosphere and radiation from the Earth) and T_R, the receiver noise temperature. Equations (1) or (3) can be used to estimate the sensitivities and interference levels for radio astronomical observations. As mentioned above, an observing (or integration) time, t, of 100 s is assumed, and interference threshold levels, ΔP_H, are expressed as the interference power within the bandwidth Δf that introduces an error of 10% in the measurement of ΔP (or ΔT), i.e.:

$$\Delta P_H = 0.1 \Delta P\, \Delta f \tag{4}$$

In summary, the appropriate columns in Tables 1 and 2 may be calculated using the following methods:

– ΔT, using equation (3),

– ΔP, using equation (2),

– ΔP_H, using equation (4).

The interference can also be expressed in terms of the pfd incident at the antenna, either in the total bandwidth or as a spectral pfd, S_H, per 1 Hz of bandwidth. The values given are for an antenna having a gain, in the direction of arrival of the interference, equal to that of an isotropic antenna (which has an effective area of $c^2/4\pi f^2$, where c is the speed of the light and f the frequency). The gain of an isotropic radiator, 0 dBi, is used as a general representative value for the side-lobe level.

Values of $S_H \Delta f$ (dB(W/m^2)) are derived from ΔP_H by adding:

$$20 \log f - 158.5 \qquad \text{dB} \tag{5}$$

where f (Hz). S_H is then derived by subtracting 10 log Δf (Hz) to allow for the bandwidth.

On the other hand, the computation for the VLBI mode is carried out following section 2.3 of Annex 1 in Recommendation ITU-R RA.769, which literally says: “The tolerable interference level is determined by the requirement that the power level of the interfering signal should be no more than 1% of the receiver noise power to prevent serious errors in the measurement of the amplitude of the cosmic signals”.

Therefore, the following equations are used to compute the maximum spectral power flux-density of the interference:

$$\Delta P_H = 0.01 \cdot k \cdot (T_A + T_R) \tag{6}$$

where:

ΔP_H : maximum tolerable RFI power

k : Boltzmann constant

T_A : antenna temperature (T_A = 12 K)

T_R : receiver temperature (T_R = 10 K).

These values for T_A and T_R have been extracted from Table 1 of Recommendation ITU-R RA.769.

Similarly, the interference in VLBI mode can also be expressed in terms of the pfd incident at the antenna, either in the total bandwidth or as a spectral pfd, S_H, per 1 Hz of bandwidth. Again, the values are computed for an antenna having a gain of 0 dBi in the direction of arrival of the interference. As before, this antenna has an effective area of $c^2/4\pi f^2$, where c is the speed of the light and f the centre frequency of the channel.

Values of $S_H \Delta f$ (dB(W/m^2)), are derived again from ΔP_H using equation (5), where f (Hz). S_H is then derived by subtracting 10 log Δf (Hz) to allow for the bandwidth.

The results are shown in Table A-2 of Annex 1, where the specific threshold levels for VLBI observations in the frequency range of VGOS (2-14 GHz), as split into 32 MHz channels, are given.

Figure 16 shows the spectral power density flux, S_v, in the VGOS frequency range for both modes, continuum and VLBI. In summary, even though operational parameters of VGOS are different to the operational parameters assumed for standard radio astronomy observations in Recommendation ITU-R RA.769, threshold levels of interference detrimental to achieve VGOS goals are similar to what can be found for continuum and VLBI within Recommendation ITU-R RA.769.

FIGURE 16

Level detrimental to achieving VGOS goals in spectral power flux-density units for the calibration process (continuum-single dish) and interferometric observations

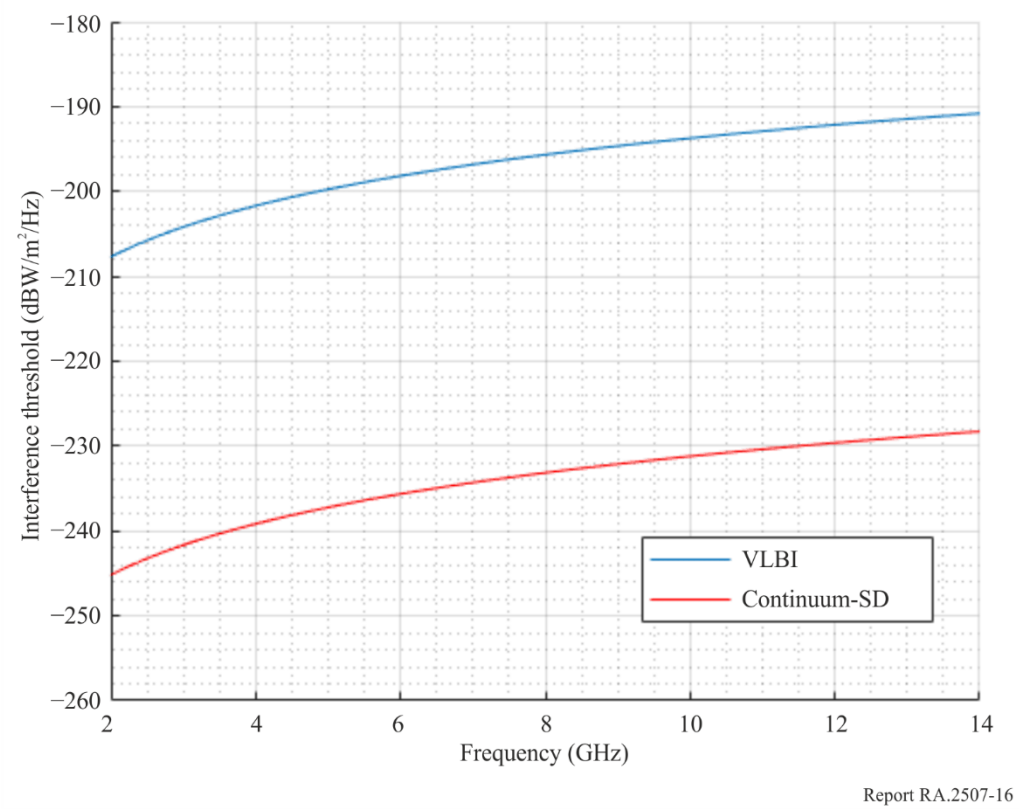

6 Summary of this Report

Geodetic VLBI observations are important to many radio services and applications which require precise positional information. Geodetic VLBI builds on the astrometric VLBI, linking the celestial reference frame with the terrestrial reference frame. The legacy VLBI systems have been routinely achieving accuracy of 10-100 mm. To achieve 1-mm or better accuracy, new VGOS systems are available and planned which include more site locations (up to ~40) and broader bandwidths in the 2-14 GHz range. VGOS utilizes this broad bandwidth as a passive user of spectrum since their operation does not interfere with any other service. Threshold levels of interference detrimental to achieve VGOS goals are similar to what can be found for continuum and VLBI within Recommendation ITU-R RA.769. To achieve desired sensitivity to reach the required positional accuracy, steps can be taken to maximize system performance.

References

[1] Thomson D.B, “Introduction to geodetic astronomy, Department of Geodesy and Geomatics Engineering”, UNB, Canada, 1997.

[2] Dehant V., “International and national geodesy and its three pillars: (1) geometry and kinematics, (2) Earth orientation and rotation, and (3) gravity field and its variability.”, in: Proc. Earth Sciences day of the CNBGG `Geodesy and geophysics for the third millennium´, Belgian Academy of Sciences, October 13, 2005, eds. E. Arijs and B. Ducarme, pp. 27-35.

[3] Niell, A., Barrett, J., Burns, A., Cappallo, R., Corey, B., Derome, M., et al., "Demonstration of a broadband very long baseline interferometer system: A new instrument for high-precision space geodesy", Radio Science, 53, 2018, https://doi.org/10.1029/2018RS006617

[4] Rogers, A. E. E., "Very long baseline interferometry with large effective bandwidth for phase-delay measurements", Radio Science, 5(10), 1239–1247, 1970, https://doi.org/10.1029/RS005i010p01239

[5] Shaffer, D.B., "RFI: Effects on Bandwidth Synthesis", IVS 2000 General Meeting Proceedings p. 402-406, 2000, http://ivscc.gsfc.nasa.gov/publications/gm2000/shaffer.pdf

[6] Ellingson, S. W., Hampson, G.A., "Mitigation Of Radar Interference In L-Band Radio Astronomy", The Astrophysical Journal Supplement Series, 147:167–176, July 2003. https://iopscience.iop.org/article/10.1086/375025/pdf

[7] Lee, K., Ellingson, S. W., Hampson, G.A., "Coherent Subtraction of Narrowband Radio Frequency Interference", Radio Science, Volume ???, Number, Pages 1–19, 2007, https://leo.phys.unm.edu/~lwa/memos/memo/lwa0085.pdf

[8] Ellingson, S. W., "Frontiers of Astronomy with the World's Largest Radio Telescope", Meeting, September 13, 2007.

[9] National Academies of Sciences, Engineering, and Medicine. 2020. *Evolving the Geodetic Infrastructure to Meet New Scientific Needs*. Washington, DC: The National Academies Press. https://doi.org/10.17226/25579.

Abbreviations/Acronyms

AU	Antenna unit
CDMS	Cable delay measurement system
COTS	Commercially available off-the-shelf
CRAF	Committee on radio astronomy frequencies
CRF	Celestial reference frame
DBBC	Digital baseband converter
EOP	Earth orientation parameters
GGOS	Global geodetic observing system
GGRF	Global geodetic reference frame
GLONASS	Global navigation satellite system
GNSS	Global navigation satellite systems
GPS	Global positioning system
HB-RA	ITU Handbook of Radio Astronomy
HTS	High-temperature superconductor
IAG	International Association of Geodesy
IAU	International Astronomical Union
ICRF	International celestial reference frame
IERS	Earth rotation and reference system service
ITRF	International terrestrial reference frame

ITU	International Telecommunication Union
IUGG	International Union of Geodesy and Geophysics
IVS	International VLBI service or geodesy and astrometry
KPGO	Kokee park geodetic observatory
LNA	Low noise amplifier
MIFR	Master International Frequency Register
RA	Radio astronomy
RAS	Radio astronomy service
RFoF	Radio frequency over fibre
SAS	Serial attached SCSI
SNR	Signal-to-noise ratio
TECU	Total electron content units (of ionosphere)
TRF	Terrestrial reference frame
TTW	Twin telescope Wettzell
UDC	Up-down converter
UN-GA	United Nations General Assembly
UT1	Universal Time: Earth rotation phase
UTC	Coordinated universal time
VDIF	VLBI data interface format
VGOS	VLBI Global Observing System
VLBA	Very Long Baseline Array
VLBI	Very Long Baseline Interferometry
VSI	VLBI Standard Interface

Annex

TABLE A.1

Threshold levels of interference detrimental to the calibration process in continuum for VGOS radio telescopes (single dish)

Start frequency (MHz)	Centre frequency (MHz)	Stop frequency (MHz)	Channel bandwidth Δf (MHz)	Antenna noise temperature T_A (K)	Receiver noise temperature T_R (K)	System sensitivity (noise fluctuations)		Threshold interference levels		
						Temperature ΔT (mK)	Power spectral density ΔP (dB(W/Hz))	Input power ΔP_H (dBW)	Power flux-density $S_H \cdot \Delta f$ (dB(W/m^2))	Spectral power-flux-density S_H (dB(W/(m^2·Hz)))
2 008.4	2 024.4	2 040.4	32	12	10	0.4	−263	−198	−170	−245
2 040.4	2 056.4	2 072.4	32	12	10	0.4	−263	−198	−170	−245
⋮	⋮	⋮	⋮	⋮	⋮	⋮	⋮	⋮	⋮	⋮
2 136.4	2 152.4	2 168.4	32	12	10	0.4	−263	−198	−170	−245
2 168.4	2 184.4	2 200.4	32	12	10	0.4	−263	−198	−169	−244
⋮	⋮	⋮	⋮	⋮	⋮	⋮	⋮	⋮	⋮	⋮
2 392.4	2 408.4	2 424.4	32	12	10	0.4	−263	−198	−169	−244
2 424.4	2 440.4	2 456.4	32	12	10	0.4	−263	−198	−168	−244
2 456.4	2 472.4	2 488.4	32	12	10	0.4	−263	−198	−168	−243
⋮	⋮	⋮	⋮	⋮	⋮	⋮	⋮	⋮	⋮	⋮
2 712.4	2 728.4	2 744.4	32	12	10	0.4	−263	−198	−167	−243
2 744.4	2 760.4	2 776.4	32	12	10	0.4	−263	−198	−167	−242
⋮	⋮	⋮	⋮	⋮	⋮	⋮	⋮	⋮	⋮	⋮
3 032.4	3 048.4	3 064.4	32	12	10	0.4	−263	−198	−167	−242
3 064.4	3 080.4	3 096.4	32	12	10	0.4	−263	−198	−166	−241
⋮	⋮	⋮	⋮	⋮	⋮	⋮	⋮	⋮	⋮	⋮
3 416.4	3 432.4	3 448.4	32	12	10	0.4	−263	−198	−165	−241
3 448.4	3 464.4	3 480.4	32	12	10	0.4	−263	−198	−165	−240

TABLE A.1 (*continued*)

Start frequency (MHz)	Centre frequency (MHz)	Stop frequency (MHz)	Channel bandwidth Δf (MHz)	Antenna noise temperature T_A (K)	Receiver noise temperature T_R (K)	System sensitivity (noise fluctuations)		Threshold interference levels		
						Temperature ΔT (mK)	Power spectral density ΔP (dB(W/Hz))	Input power ΔP_H (dBW)	Power flux-density $S_H \cdot \Delta f$ (dB(W/m^2))	Spectral power-flux-density S_H (dB(W/(m^2·Hz)))
⋮	⋮	⋮	⋮	⋮	⋮	⋮	⋮	⋮	⋮	⋮
3 832.4	3 848.4	3 864.4	32	12	10	0.4	−263	−198	−164	−240
3 864.4	3 880.4	3 896.4	32	12	10	0.4	−263	−198	−164	−239
⋮	⋮	⋮	⋮	⋮	⋮	⋮	⋮	⋮	⋮	⋮
4 312.4	4 328.4	4 344.4	32	12	10	0.4	−263	−198	−163	−239
4 344.4	4 360.4	4 376.4	32	12	10	0.4	−263	−198	−163	−238
⋮	⋮	⋮	⋮	⋮	⋮	⋮	⋮	⋮	⋮	⋮
4 824.4	4 840.4	4 856.4	32	12	10	0.4	−263	−198	−163	−238
4 856.4	4 872.4	4 888.4	32	12	10	0.4	−263	−198	−162	−237
⋮	⋮	⋮	⋮	⋮	⋮	⋮	⋮	⋮	⋮	⋮
5 432.4	5 448.4	5 464.4	32	12	10	0.4	−263	−198	−161	−237
5 464.4	5 480.4	5 496.4	32	12	10	0.4	−263	−198	−161	−236
⋮	⋮	⋮	⋮	⋮	⋮	⋮	⋮	⋮	⋮	⋮
6 104.4	6 120.4	6 136.4	32	12	10	0.4	−263	−198	−160	−236
6 136.4	6 152.4	6 168.4	32	12	10	0.4	−263	−198	−160	−235
⋮	⋮	⋮	⋮	⋮	⋮	⋮	⋮	⋮	⋮	⋮
6 808.4	6 824.4	6 840.4	32	12	10	0.4	−263	−198	−160	−235
6 840.4	6 856.4	6 872.4	32	12	10	0.4	−263	−198	−159	−235
6 872.4	6 888.4	6 904.4	32	12	10	0.4	−263	−198	−159	−234
⋮	⋮	⋮	⋮	⋮	⋮	⋮	⋮	⋮	⋮	⋮
7 640.4	7 656.4	7 672.4	32	12	10	0.4	−263	−198	−159	−234
7 672.4	7 688.4	7 704.4	32	12	10	0.4	−263	−198	−158	−234

TABLE A.1 (*continued*)

Start frequency (MHz)	Centre frequency (MHz)	Stop frequency (MHz)	Channel bandwidth Δf (MHz)	Antenna noise temperature T_A (K)	Receiver noise temperature T_R (K)	System sensitivity (noise fluctuations)		Threshold interference levels		
						Temperature ΔT (mK)	Power spectral density ΔP (dB(W/Hz))	Input power ΔP_H (dBW)	Power flux-density $S_H \cdot \Delta f$ (dB(W/m^2))	Spectral power-flux-density S_H (dB(W/(m^2·Hz)))
7 704.4	7 720.4	7 736.4	32	12	10	0.4	−263	−198	−158	−233
⋮	⋮	⋮	⋮	⋮	⋮	⋮	⋮	⋮	⋮	⋮
8 568.4	8 584.4	8 600.4	32	12	10	0.4	−263	−198	−158	−233
8 600.4	8 616.4	8 632.4	32	12	10	0.4	−263	−198	−157	−233
8 632.4	8 648.4	8 664.4	32	12	10	0.4	−263	−198	−157	−233
8 664.4	8 680.4	8 696.4	32	12	10	0.4	−263	−198	−157	−232
⋮	⋮	⋮	⋮	⋮	⋮	⋮	⋮	⋮	⋮	⋮
9 624.4	9 640.4	9 656.4	32	12	10	0.4	−263	−198	−157	−232
9 656.4	9 672.4	9 688.4	32	12	10	0.4	−263	−198	−156	−232
9 688.4	9 704.4	9 720.4	32	12	10	0.4	−263	−198	−156	−232
9 720.4	9 736.4	9 752.4	32	12	10	0.4	−263	−198	−156	−231
⋮	⋮	⋮	⋮	⋮	⋮	⋮	⋮	⋮	⋮	⋮
10 808.4	10 824.4	10 840.4	32	12	10	0.4	−263	−198	−156	−231
10 840.4	10 856.4	10 872.4	32	12	10	0.4	−263	−198	−155	−231
10 872.4	10 888.4	10 904.4	32	12	10	0.4	−263	−198	−155	−231
10 904.4	10 920.4	10 936.4	32	12	10	0.4	−263	−198	−155	−230
⋮	⋮	⋮	⋮	⋮	⋮	⋮	⋮	⋮	⋮	⋮
12 120.4	12 136.4	12 152.4	32	12	10	0.4	−263	−198	−155	−230
12 152.4	12 168.4	12 184.4	32	12	10	0.4	−263	−198	−154	−230
12 184.4	12 200.4	12 216.4	32	12	10	0.4	−263	−198	−154	−230
12 216.4	12 232.4	12 248.4	32	12	10	0.4	−263	−198	−154	−230

TABLE A.1 (*end*)

Start frequency (MHz)	**Centre frequency** (MHz)	**Stop frequency** (MHz)	**Channel bandwidth** Δf (MHz)	**Antenna noise temperature** T_A (K)	**Receiver noise temperature** T_R (K)	**System sensitivity (noise fluctuations)**		**Threshold interference levels**		
						Temperature ΔT (mK)	**Power spectral density** ΔP (dB(W/Hz))	**Input power** ΔP_H (dBW)	**Power flux-density** $S_H \cdot \Delta f$ (dB(W/m^2))	**Spectral power-flux-density** S_H (dB(W/(m^2·Hz)))
12 248.4	12 264.4	12 280.4	32	12	10	0.4	−263	−198	−154	−229
⋮	⋮	⋮	⋮	⋮	⋮	⋮	⋮	⋮	⋮	⋮
13 624.4	13 640.4	13 656.4	32	12	10	0.4	−263	−198	−154	−229
13 656.4	13 672.4	13 688.4	32	12	10	0.4	−263	−198	−153	−229
13 688.4	13 704.4	13 720.4	32	12	10	0.4	−263	−198	−153	−229
13 720.4	13 736.4	13 752.4	32	12	10	0.4	−263	−198	−153	−228
⋮	⋮	⋮	⋮	⋮	⋮	⋮	⋮	⋮	⋮	⋮
13 976.4	13 992.4	14 008.4	32	12	10	0.4	−263	−198	−153	−228

TABLE A.2

Threshold levels of interference detrimental to VLBI observations for VGOS radiotelescopes

Start frequency (MHz)	Centre frequency (MHz)	Stop frequency (MHz)	Channel bandwidth Δf (MHz)	Antenna noise temperature T_A (K)	Receiver noise temperature T_R (K)	Threshold interference levels		
						Input power ΔP_H (dBW)	Power flux-density $S_H \cdot \Delta f$ (dB(W/m^2))	Spectral power flux-density S_H (dB(W/(m^2·Hz)))
2 008.4	2 024.4	2 040.4	32	12	10	−235	−133	−208
2 040.4	2 056.4	2 072.4	32	12	10	−235	−132	−207
⋮	⋮	⋮	⋮	⋮	⋮	⋮	⋮	⋮
2 264.4	2 280.4	2 296.4	32	12	10	−235	−132	−207
2 296.4	2 312.4	2 328.4	32	12	10	−235	−131	−206
⋮	⋮	⋮	⋮	⋮	⋮	⋮	⋮	⋮
2 552.4	2 568.4	2 584.4	32	12	10	−235	−130	−206
2 584.4	2 600.4	2 616.4	32	12	10	−235	−130	−205
⋮	⋮	⋮	⋮	⋮	⋮	⋮	⋮	⋮
2 872.4	2 888.4	2 904.4	32	12	10	−235	−129	−205
2 904.4	2 920.4	2 936.4	32	12	10	−235	−129	−204
⋮	⋮	⋮	⋮	⋮	⋮	⋮	⋮	⋮
3 192.4	3 208.4	3 224.4	32	12	10	−235	−129	−204
3 224.4	3 240.4	3 256.4	32	12	10	−235	−128	−204
3 256.4	3 272.4	3 288.4	32	12	10	−235	−128	−203
⋮	⋮	⋮	⋮	⋮	⋮	⋮	⋮	⋮
3 576.4	3 592.4	3 608.4	32	12	10	−235	−128	−203
3 608.4	3 624.4	3 640.4	32	12	10	−235	−127	−203
3 640.4	3 656.4	3 672.4	32	12	10	−235	−127	−202

TABLE A.2 (*continued*)

Start frequency (MHz)	Centre frequency (MHz)	Stop frequency (MHz)	Channel bandwidth Δf (MHz)	Antenna noise temperature T_A (K)	Receiver noise temperature T_R (K)	Threshold interference levels		
						Input power ΔP_H (dBW)	Power flux-density $S_H \cdot \Delta f$ (dB(W/m^2))	Spectral power flux-density S_H (dB(W/(m^2·Hz)))
⋮	⋮	⋮	⋮	⋮	⋮	⋮	⋮	⋮
4 024.4	4 040.4	4 056.4	32	12	10	−235	−127	−202
4 056.4	4 072.4	4 088.4	32	12	10	−235	−126	−202
4 088.4	4 104.4	4 120.4	32	12	10	−235	−126	−201
⋮	⋮	⋮	⋮	⋮	⋮	⋮	⋮	⋮
4 536.4	4 552.4	4 568.4	32	12	10	−235	−126	−201
4 568.4	4 584.4	4 600.4	32	12	10	−235	−125	−200
⋮	⋮	⋮	⋮	⋮	⋮	⋮	⋮	⋮
5 080.4	5 096.4	5 112.4	32	12	10	−235	−125	−200
5 112.4	5 128.4	5 144.4	32	12	10	−235	−124	−200
5 144.4	5 160.4	5 176.4	32	12	10	−235	−124	−199
⋮	⋮	⋮	⋮	⋮	⋮	⋮	⋮	⋮
5 720.4	5 736.4	5 752.4	32	12	10	−235	−124	−199
5 752.4	5 768.4	5 784.4	32	12	10	−235	−123	−199
5 784.4	5 800.4	5 816.4	32	12	10	−235	−123	−198
⋮	⋮	⋮	⋮	⋮	⋮	⋮	⋮	⋮
6 392.4	6 408.4	6 424.4	32	12	10	−235	−123	−198
6 424.4	6 440.4	6 456.4	32	12	10	−235	−122	−198
6 456.4	6 472.4	6 488.4	32	12	10	−235	−122	−198
6 488.4	6 504.4	6 520.4	32	12	10	−235	−122	−197

TABLE A.2 (*continued*)

Start frequency (MHz)	Centre frequency (MHz)	Stop frequency (MHz)	Channel bandwidth Δf (MHz)	Antenna noise temperature T_A (K)	Receiver noise temperature T_R (K)	Threshold interference levels		
						Input power ΔP_H (dBW)	Power flux-density $S_H \cdot \Delta f$ (dB(W/m^2))	Spectral power flux-density S_H (dB(W/(m^2·Hz)))
⋮	⋮	⋮	⋮	⋮	⋮	⋮	⋮	⋮
7 192.4	7 208.4	7 224.4	32	12	10	−235	−122	−197
7 224.4	7 240.4	7 256.4	32	12	10	−235	−121	−197
7 256.4	7 272.4	7 288.4	32	12	10	−235	−121	−196
⋮	⋮	⋮	⋮	⋮	⋮	⋮	⋮	⋮
8 056.4	8 072.4	8 088.4	32	12	10	−235	−121	−196
8 088.4	8 104.4	8 120.4	32	12	10	−235	−120	−196
8 120.4	8 136.4	8 152.4	32	12	10	−235	−120	−196
8 152.4	8 168.4	8 184.4	32	12	10	−235	−120	−195
⋮	⋮	⋮	⋮	⋮	⋮	⋮	⋮	⋮
9 048.4	9 064.4	9 080.4	32	12	10	−235	−120	−195
9 080.4	9 096.4	9 112.4	32	12	10	−235	−119	−195
9 112.4	9 128.4	9 144.4	32	12	10	−235	−119	−195
9 144.4	9 160.4	9 176.4	32	12	10	−235	−119	−194
⋮	⋮	⋮	⋮	⋮	⋮	⋮	⋮	⋮
10 168.4	10 184.4	10 200.4	32	12	10	−235	−119	−194
10 200.4	10 216.4	10 232.4	32	12	10	−235	−118	−194
10 232.4	10 248.4	10 264.4	32	12	10	−235	−118	−194
10 264.4	10 280.4	10 296.4	32	12	10	−235	−118	−193

TABLE A.2 (*end*)

Start frequency (MHz)	**Centre frequency** (MHz)	**Stop frequency** (MHz)	**Channel bandwidth** Δf (MHz)	**Antenna noise temperature** T_A (K)	**Receiver noise temperature** T_R (K)	**Threshold interference levels**		
						Input power ΔP_H (dBW)	**Power flux-density** $S_H \cdot \Delta f$ (dB(W/m^2))	**Spectral power flux-density** S_H (dB(W/(m^2·Hz)))
⋮	⋮	⋮	⋮	⋮	⋮	⋮	⋮	⋮
11 416.4	11 432.4	11 448.4	32	12	10	−235	−118	−193
11 448.4	11 464.4	11 480.4	32	12	10	−235	−117	−193
11 480.4	11 496.4	11 512.4	32	12	10	−235	−117	−193
11 512.4	11 528.4	11 544.4	32	12	10	−235	−117	−192
⋮	⋮	⋮	⋮	⋮	⋮	⋮	⋮	⋮
12 824.4	12 840.4	12 856.4	32	12	10	−235	−117	−192
12 856.4	12 872.4	12 888.4	32	12	10	−235	−116	−192
12 888.4	12 904.4	12 920.4	32	12	10	−235	−116	−192
12 920.4	12 936.4	12 952.4	32	12	10	−235	−116	−191
⋮	⋮	⋮	⋮	⋮	⋮	⋮	⋮	⋮
13 976.4	13 992.4	14 008.4	32	12	10	−235	−116	−191